Light Collection Efficiency Map of the XENON100 Detector

Therreau Chloé

Project Supervisor: Prof. Dr. M.P Decowski

Nikhef- National institute for subatomic physics

Science Park 105

1098 XG Amsterdam

Nikhef

UNIVERSITÉ DE NANTES

Résumé

Depuis la fin du dernier siècle, plusieurs observations astrophysiques ont montré qu'une grande partie de la masse de l'univers est composée d'une substance que l'on ne peut détecter, appelée la matière noire. Ces observations ont, en réalité, montré que 85% de la masse de l'univers est sous forme de matière noire. Depuis, les physiciens ont développé plusieurs expériences pour détecter cette matière « invisible ». Même si la matière noire n'a toujours pas été découverte, la sensibilité de ces expériences de détection a été grandement améliorée [4]. De nouvelles expériences, avec une plus grande sensibilité, doivent voir le jour dans les prochaines décennies.

L'expérience XENON100 est une expérience de détection direct de la matière noire qui utilise du xénon liquide pour détecter des interactions entre une particule de matière noire et un atome de xénon. Pendant deux mois, j'ai travaillé sur l'analyse de données de cette expérience.

Ce rapport est une introduction à la matière noire et en particulier, une présentation de l'expérience XENON100. Je présente également mon travail effectué sur l'analyse de données du détecteur XENON100 qui a permit une calibration du rendement de la scintillation et de la charge du détecteur avec une source de Cs-137 à 662 keV.

Abstract

In the last century, several astrophysical observations showed that a large part of the universe's mass is composed of something we have not detected until now: dark matter. Actually, these observations showed that 85% of the mass of the universes is dark matter. Since these observations, physicists had developed several experiments to detect this "invisible" matter. Even if dark matter has not been discovered yet, the sensitivity of direct and indirect detection experiments has been highly improved in the past decade [4]. New experiments with a greater sensitivity are planned for the next decade.

The XENON100 Experiment is a direct detection experiment using liquid xenon in a time projection chamber to detect interactions between a dark matter particle and a xenon atom. For two months, I worked on the data analysis of XENON100.

This paper is an introduction to dark matter and more precisely a presentation of the XENON100 experiment. I also present my work on the data analysis of the XENON100 detector that allow me to calibrate both the scintillation and charge yield in XENON100 with a Cs-137 source at 662 KeV.

Contents

1 Introduction

1.1 Presentation of Nikhef

Nikhef, the national institute for subatomic physics is located in Science Park Amsterdam, in the Netherlands. Nikhef is lead by Stan Bentvelsen since 2014.

Nikhef is a partnership between the Foundation for Fundamental Research on Matter (FOM), which is part of the Netherlands Organization for Scientific Research, and five universities: Radboud University, the University of Groningen, the University of Amsterdam, Utrecht University and VU University. The name of Nikhef originates from the name “National Institute for Nuclear Physics and High Energy Physics”.

The Nikhef's primary mission is to coordinate and lead the Dutch experimental activities on particle and astroparticle physics with 10 different research groups:

- Astrophysics groups: Dark Matter, Cosmic Rays, Neutrino Telescopes and Gravitational Waves.

- Particle physics groups: ALICE, ATLAS and LHCb (All three are LHC experiments).

- Other research projects groups: Detector R&D, Grid Computing and Theoretical Physics.

Knowledge and technology transfer is another one of Nikhef's missions [11]. I did my internship in the dark matter group lead by Patrick Decowski. This group is a part of the XENON project which is a collaboration of 21 institutions across the world and representing 24 nationalities. The XENON collaboration is trying to detect dark matter.

1.2 Presentation of the internship

During this internship, I worked on the data analysis of the XENON100 experiment under the supervision of two PhD students: Sander Breur and Erik Hogenbirk. On part 2, you will find an introduction of what is dark matter. On part 3, I studied the XENON100 detector and the data analysis software used in the dark matter group. On part 4, I analyzed data taken with a radioactive Cesium source placed next to the detector, improved the energy resolution, and worked on the light collection efficiency map of the XENON detector.

One of the main objectives of this internship was to learn how to work in a team. Indeed, I had the opportunity to attend group meetings every week. I also had to make several presentations of the progress of my work in front of the entire group during these meetings. In addition, I had the opportunity to work with others students on the data analysis of the new dark matter experiment: XENON1T.

2 Dark matter

2.1 What is dark matter?

The existence of dark matter was introduced to explain several astrophysics observations which indicate the presence of a missing mass in the universe. The distribution of the universe's mass is represented in the Fig.1 [1]

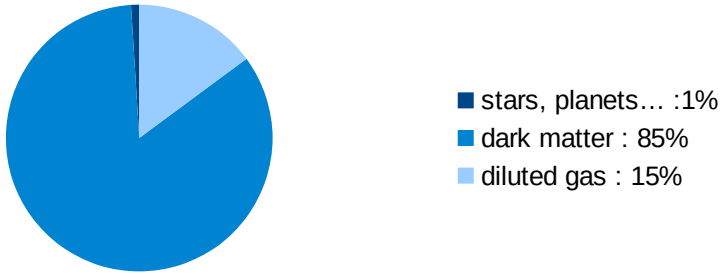

Fig. 1: Distribution of the universe's mass [1]. 85 % of the universe's mass is dark matter.

One of these is the observation of the rotational velocity distribution of spirals galaxies.

Stars rotate around the center of the galaxy. The rotational velocity of these stars is related to the gravitational force and therefore related to the mass of the galaxy. Indeed, the velocity is related to the centripetal force which compensates the gravitational force. If we take the example of a galaxy which has the major part of its mass in its center, we should see the velocity of the stars decreases when the distance between the star and the center of the galaxy increases. However, the measurements of the rotational velocity as a function of the distance between stars and the center of the galaxy do not give this theoretical repartition as shown in Fig.2.

Fig.2 shows a large discrepancy between observation and theory. The experimental rotation curves are “flat”, indicating that the rotational velocity of stars is roughly constant with the distance between stars and the center of the galaxy. The gravitational force required for these rotational velocities must come from an unknown form of massive matter that surrounds each galaxy: dark matter.

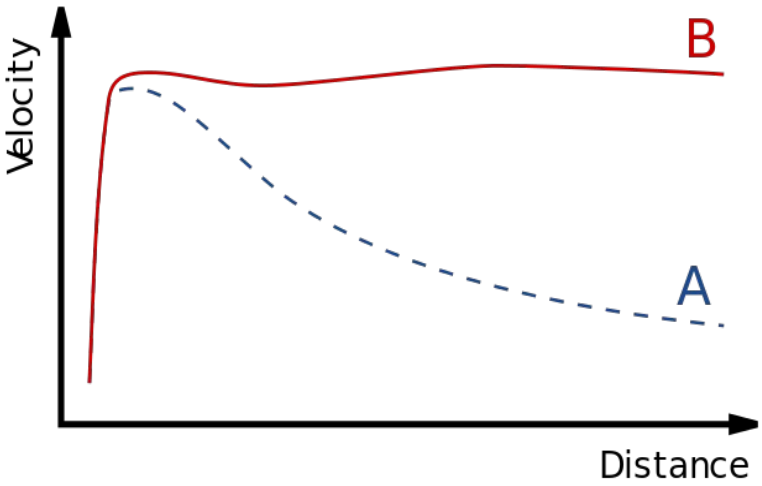

A : theoretical curve based on the visible mass of the galaxy

B: curve based on observations

Fig. 2:Shape of rotational curve of a typical spiral galaxy [2]. “Distance” is the distance of stars from the center of the galaxy. “Velocity” is the rotational velocity of stars. The difference between theoretical and observed curve is caused by a dark matter halo that surrounds the galaxy.

There are other arguments that imply the existence of a missing mass in the universe like the gravitational lens effect. This effect is caused by the bending of light by a massive object. Thanks to it, the quantity of galaxies' mass can be directly measured, showing the existence of missing matter in the universe [1][3].

If we consider dark matter exists, the next question is: what is this dark matter made of? One of the theory is that dark matter is composed of particles. According to what we just said, these particles have certain properties:

- be massive (to explain that 85% the universe's mass is dark matter)
- have a neutral charge (charged particles are easy to detect by their interactions with standard matter)
- be weakly interacting (otherwise scientists would have already detect them by their interactions with particles of the standard model).

The Weakly Interactive Massive Particles (WIMPs) are candidates for playing the role of dark matter particles.

2.2 Detection of dark matter

Several scientific collaborations have tried to prove the existence of dark matter by three different ways: indirect detection, direct detection and production at colliders.

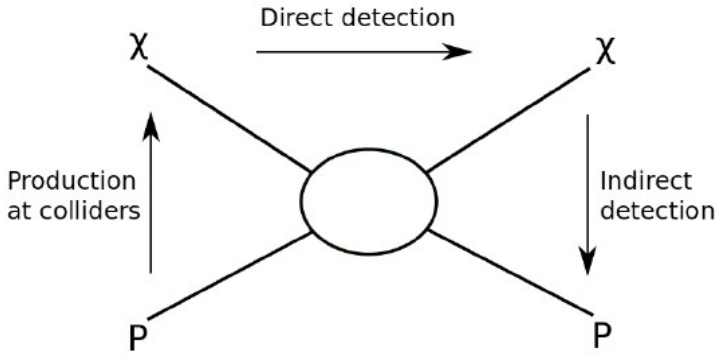

Fig. 3: Schematic of interaction process showing the possible dark matter detection channels [4]. χ : dark matter particle ; P : standard model particle. The arrows show the direction of reactions.

Fig.3 can be represented as:

Direct detection: $p+\chi \rightarrow p+\chi$ (2.1)

Indirect detection: $\chi+\chi \rightarrow p+\bar{p}$ (2.2)

Production: $p+\bar{p} \rightarrow \chi+\chi$ (2.3)

where $\bar{p}$ *is the antiparticle of* p

2.2.1 Production

One way to detect dark matter is to create it in colliders like the LHC, based on (2.3). Because dark matter particles would interact weakly, they pass through the detector without interacting. However, these particles have an energy. This energy taken by dark matter is "missing" when the total expected energy is compared to the total measured energy. A difference like this would thus indicate the existence of dark matter.

2.2.2 Indirect Detection

Indirect detection is based on the fact that dark matter particles can interact with each others and can be annihilated in standard model particles, such as γ-rays, based on (2.2).
However, the dark matter density is low, and therefore, the annihilation of two dark matter particles have a very low probability. Besides, γ-rays are very common in the universe. That is why scientists have to look at area of the universe where dark matter is dense (to increase the probability of interaction) and where the background created by γ-rays is low [5]. VERITAS, HESS, MAGIC (and many others [6]) are examples of indirect detection experiments.

2.2.3 Direct Detection

The earth is in our galaxy, the Milky Way, and like all the other galaxies in the universe, the Milky Way should be surrounded by a halo of dark matter. When the earth rotates around the Sun which also moves in the galaxy, particles of dark matter pass through the earth. Direct detection experiments try to "see" collisions between dark matter particles and standard model particles based on (2.1).

However, it is difficult to detect a collision between a detector and dark matter particles for several reasons:

1) Dark matter particles are weakly interacting. There are very few collisions between them and the detector.

2) The background from cosmic rays is high compared to the expected event rate for dark matter. That is why this detector is placed deep underground (to shield it from cosmic radiation). Also other issues appear: the natural radioactivity of the ground, of the detector materials and the intrinsic detector radioactivity emit standard model particles (such as γ-rays, α and β particles..). All these particles will interact with the detector. Cosmic radiation and natural radioactivity is most of the background signal. To avoid this background, radio-pure materials (with low uranium and thorium contents) and a large detector shielding are used. [4]

3) Even if the background is significantly reduced, some particles (like neutrons) can go through the shielding and interact with the detector. To discriminate neutrons from WIMPs, we have to use knowledge about the expected WIMP signal.

   - Because of the sun's rotation around the center of the galaxy and the rotation of the earth

around the sun, the velocity of the earth in the halo of dark matter changes during the year: in June the Earth's velocity will add to the sun's velocity whereas in December, the velocities are opposite. Therefore, the flux of dark matter particles should be maximal in June and minimal in December [7][3]. Dark matter should thus have a yearly modulation, while the background signal should stay the same.

- Collisions between dark matter and detector give three ways of possible signals (Fig.4): production of heat as phonon, scintillation (light produced by excitation and subsequent de-excitation of the target nucleus) and ionization of atoms (electrons). Direct detection experiments usually use two of these three possible signals [4][8].

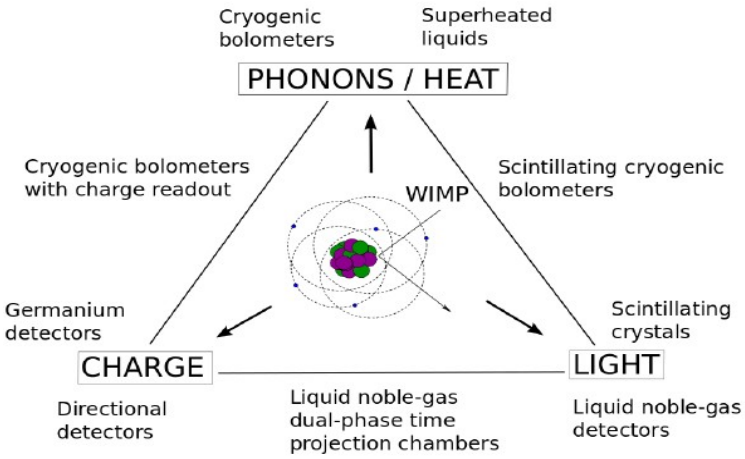

Fig. 4: Schematic of possibles signals that can be measured in direct detection experiments depending on the technology in use [4]

CDMS (Germanium detector and silicon bolometers), DAMA (scintillation crystals), DarkSide (liquid argon), XENON (liquid xenon) are examples of direct detection experiments [8].

3 The XENON100 experiment

3.1 Description of the detector

The XENON100 detector is placed at the Laboratori Nazionai del Gran Sasso, in Italy. It is a cylindrical dual phase time-projection chamber (TPC) with an active target of 62 kg of liquid xenon with a layer of xenon gas above it and 242 photomultiplier tubes (PMTs) divided between two arrays [10].

3.1.1 Liquid Xenon

Liquid xenon was chosen for this experiment for several reasons. First, it gives a homogeneous target with a large density that increases the probability of interactions with a dark matter particle. Secondly, liquid xenon has a high ionization and scintillation (de-excitation of an atoms) yield. In addition, the scintillation light of xenon has a wavelength of 175 nm and therefore can be directly detected using PMTs (sensitive to ultraviolet light) [4] [11]. Liquid xenon is also transparent to its scintillation light and has a low intrinsic radiation.

3.1.2 Photomultiplier tubes

A photomultiplier tube (PMT) is a vacuum tube made of a photocathode, several dynodes and an anode. PMTs are used to detect photons (from the ultraviolet to the infrared, depending on the material used). When a photon hits the photocathode, an electron is produce by the photoelectric effect. When this first electron hits the first dynode, more electrons are emitted and these electrons hit the second dynode. Finally, the electrons at the output have enough charge to produce a measurable signal [14]

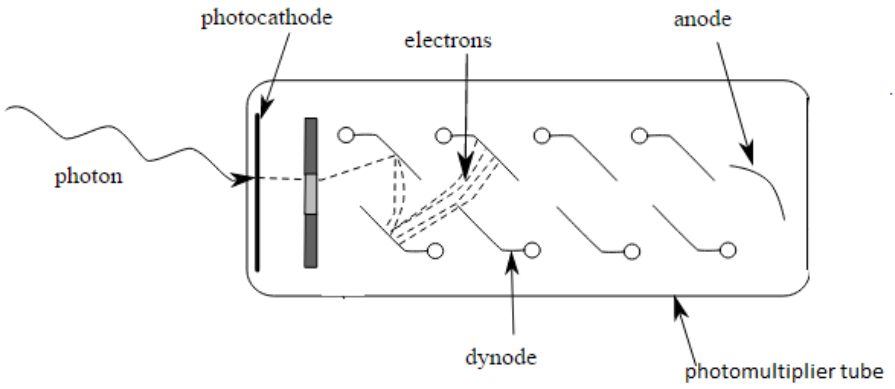

Fig. 5: Scheme of a photomultiplier tube [15]. Photons generate electrons by photoelectric effect on the photocathode. A series of dynode amplifies the signal till they reach the anode where the signal can be readout.

3.1.3 The dual phase time projection chamber

When a particle (γ-ray or WIMP for example) hits the liquid xenon, xenon atoms are ionized and excited. The excited xenon atoms will from with an other xenon atom an excited state that will decay to the ground state. During this de-excitation, the first scintillation signal, S1, is emitted. The S1 signal can be directly detected by the photomultiplier tubes. At the same time, some of the electrons coming from the ionization of xenon are guided to the gas phase by an electrical field. A second stronger electrical field extracts the electrons from the liquid phase to the gas phase, generating a light signal: the secondary scintillation signal, called S2 [9][13].

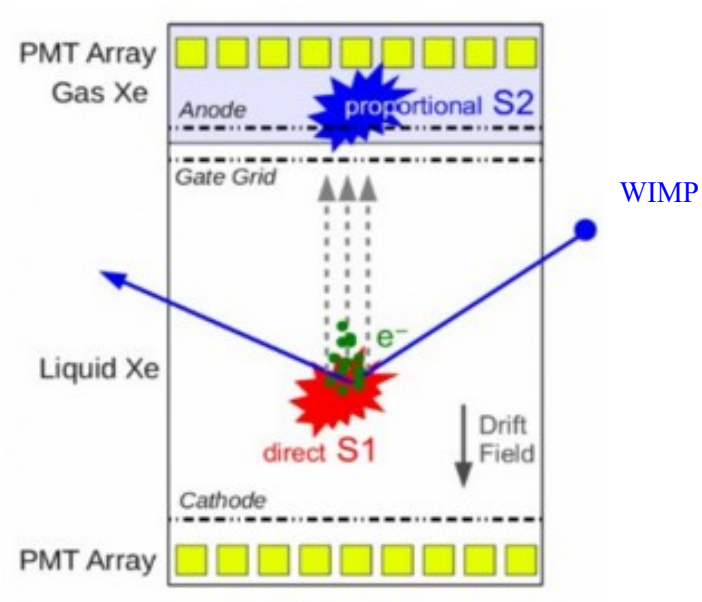

Fig. 6: Functional principal of the XENON100 detector [9]. A WIMP interact with liquid xenon in the TPC, generating S1 and S2 signals. S1 is emitted during the de-excitation of the liquid xenon. A drift field guides the electrons (coming from the ionization of the liquid xenon) to the gas phase, generating S2.

One of the advantages of using a time projection chamber is that this detector allows a 3-dimensional reconstruction of the interaction. The x-y position is determined by the S2 signal (x-y positions are the position of the interaction on the TPC viewed from above). The S2 signal is at the same x-y position that the interaction, and is close to the top PMT array. Thereby, the position of the S2 signal in the top PMT array gives a precise x-y position. The z position is determined by the time difference between the S1 and the S2 signal, called the drift time which is proportional to the distance travelled on the TPC [15].

Another advantage is that the time projection chamber allows us to discriminate a WIMP interaction from other particle interactions. Indeed, the ratio of S1 and S2 signals has not the same

characteristics if S1 and S2 signals come from an interaction between liquid xenon and a WIMPs or if they come from an interaction between liquid xenon and a standard model particle, such as γ-rays or β particles..). WIMPs (and neutrons) are expected to a cause nuclear recoil in the liquid xenon while γ-ray (for example) cause an electronic recoil. Thereby, WIMP and γ-ray do not product the same ratio between the light and the ionization as shown in Fig.7.

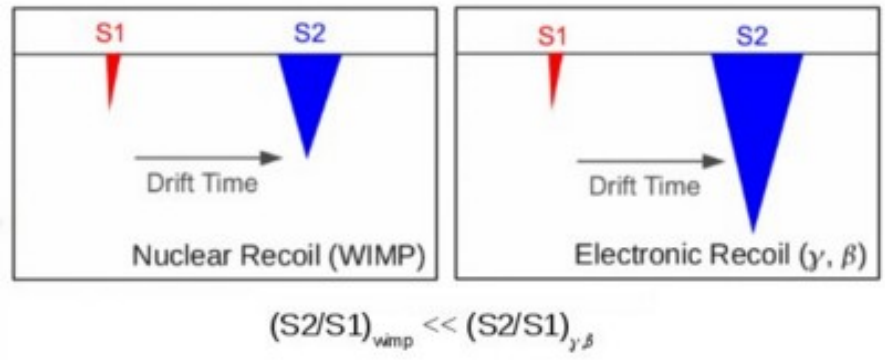

Fig. 7: Signal difference between WIMP interaction and background noise interaction [9]. Electronic and Nuclear recoil do not give the same S1-S2 ratio, allowing discrimination between WIMPs and background signal.

Others methods are used to reduce the background. A large shielding surrounds the detector, as shown in Fig.8. It is placed 10 000 meters under the Gran Sasso mountain in Italy to reduce the cosmic radiation background [11]. Secondly, the detector is encircled with 99kg of liquid xenon used as an active scintillator veto (to ignore a signal created by a cosmic radiation). The detector is also placed into a cryostat, surround by layer of copper, polyethylene, lead and water [13]. Finally, since the time-projection chamber permits the positioning of the interaction, the radioactivity background can be reduce knowing that radioactivity background is most likely at the edge of the detector [9].

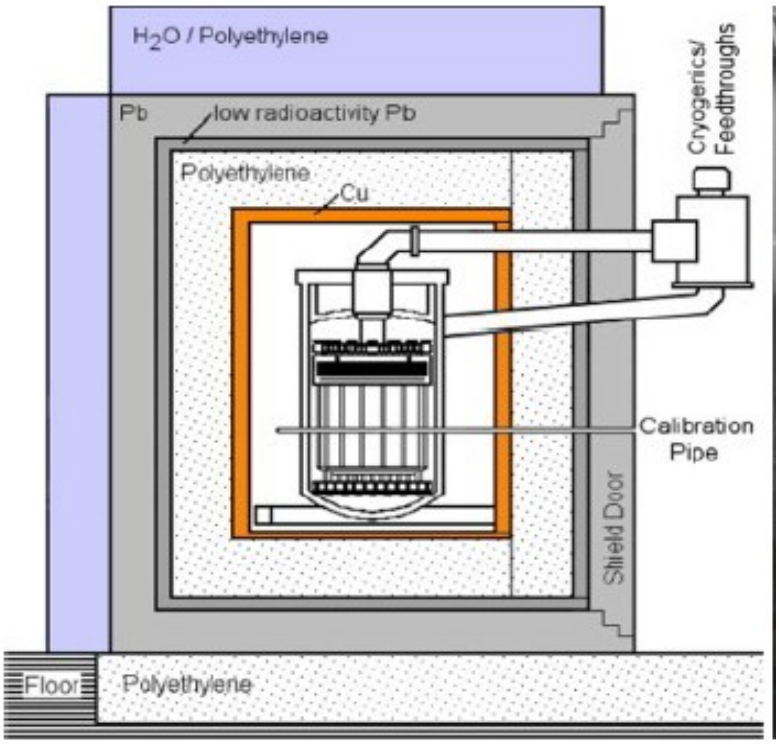

Fig. 8: Shielding of the XENON100 detector [13]. The TPC filled of xenon is placed into a cryostat, surrounded by layer of copper, polyethylene, lead and water to reduce the background.

3.2 Data analysis software used in Nikhef

Since the XENON detector is composed of 242 photomultiplier tubes (PMTs), it collects a lot of raw data.

When a PMT detects a photon, a pulse can be observed surrounded by a baseline. A digitizer permits to exclude the baseline from the data, leaving only the pulses. At this point, the data is composed of a lot of pulses coming from each PMT. To organize this raw data, we use PAX (Processor for Analyzing XENON). PAX finds the hits of each pulse for each PMT. After that, PAX clusters the hits in peaks then it computes and classifies the properties of each peaks, given S1 peaks or S2 peaks. Here, PAX creates a ROOT file containing our processed data, as shown in Fig.10. Afterward, HAX (Handy Analysis tools for XENON) allows us to extract data from the ROOT file and make small ones (called miniTree) which contain just the data we want to analyze [16]. A basic minitree is automatically created when we use HAX. If we want other information, we have to create our own minitree that will call information contain in the “pax event class”: http://xenon1t.github.io/pax/format.html

Fig. 9: Pax logo

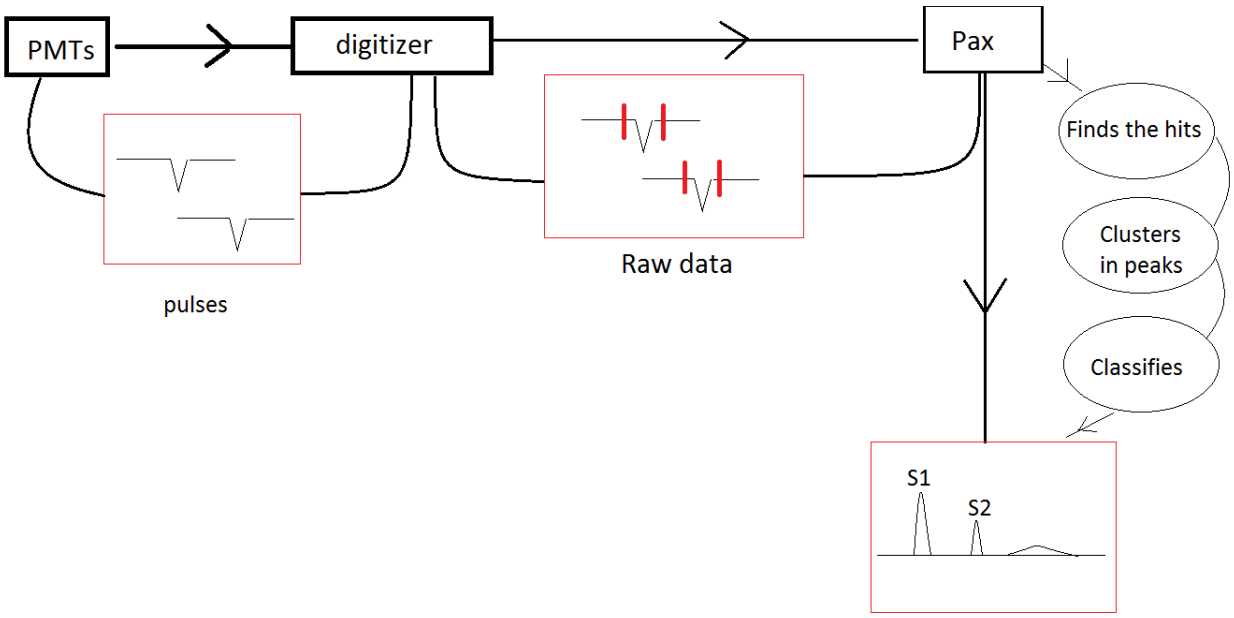

Fig. 10: Functional schema of PAX. The data flow are pulses surrounded by a baseline. A digitizer permits to exclude the baseline from the data, leaving only the pulses. Then, the data are processed by PAX.

4 Light Collection Efficiency Map

During my internship, I analyzed data taken with a radioactive Cesium source placed next to the XENON100 detector. These data are used to calibrate the detector and create a light collection efficiency map.

4.1 Why do we need a S1 light collection efficiency map?

For a given energy deposition, the quantity of scintillation light measured depends on the position of the interaction in the time projection chamber (we will prove it with our data in part 4). There are several effects that affect the light collection efficiency, for example:

- The impurities: a photon emitted after an interaction can be absorbed by impurities in the xenon, reducing the observed signal.

- The solid angle effect: if photons are emitted close to the PMT array, the solid angle covered by these PMT becomes smaller, reducing the observed signal.

- The reflectivity of the TPC: when an interaction occurs, photons go in all directions and can be reflected by the wall of the TPC and therefore can distort the data when reflected photons hit the PMTs.

- The Rayleigh scattering: an elastic scattering of light occurs when the radiation hits particles smaller than its wavelength. The scattered photon has a lower energy and thus gives a smaller measured energy.

These effects, that affect the S1 signal, depend on the properties of the detector and are the reason why we need a map of the light collection efficiency to correct the data. To make this map, several radioactive sources were used and placed at different positions around the detector [15] [17]. An example of this map, from previous analysis of XENON100, is shown in Fig.11.

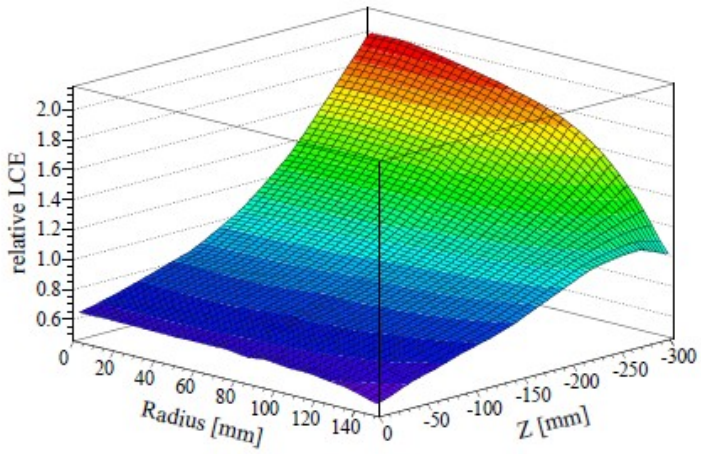

Fig. 11: Correction map for the light collection efficiency. The measured S1 signals are divided by the values from this map [15].

4.2 Cesium source

4.2.1 Cesium 137

In the remainder of the paper, we will analyze data taken with ^{137} Cs source placed next to the detector. The Cesium-137 is a radioactive isotope with a half-live of roughly 30 years. The ^{137}Cs is a β- emitter. It decays, with a probability of 94,6%, to a metastable state of Barium-137m. The ^{137m} Ba has a half-life of 2,5 min. When it decays to its stable state, it emits a γ-ray with an energy of 661,7 keV [18]. These γ-rays will interact in the liquid xenon.

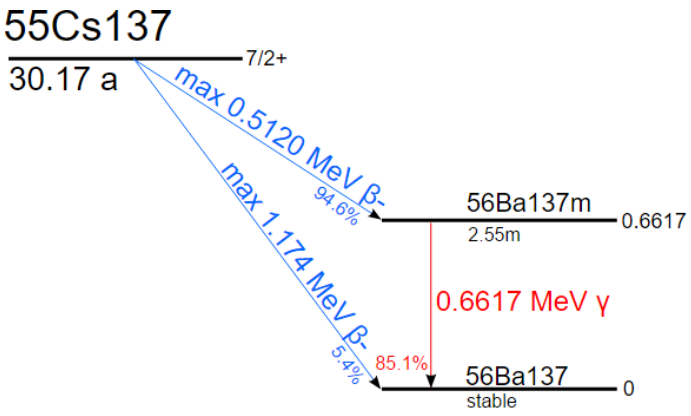

Fig. 12: Cs137 decay scheme [18]. A γ-ray with a energy of 661,7 keV is emitted.

4.2.2 Photoelectric and Compton effect

When a γ-ray interacts with an atom, several effect can occur: the photoelectric effect, Compton scattering and pair production (if the initial γ-ray has an energy superior to 1,022 MeV). With a Cesium source, γ-rays are emitted with an energy of 661,7 keV: the pair production can not happen.

The photoelectric effect occurs when a γ-ray collides with an electron of the detector material. This electron is ejected and takes all the energy of the photon. In the case of the XENON100 detector, the ejected electron will excite and ionize xenon atoms, generating S1 and S2 signals. The measured energy spectrum of S1 and S2 will have a photoelectric peak at the energy of the initial γ-ray, as shown in Fig.13. For the Cesium source, we expected a photoelectric peak at 661,7 keV.

In this case of Compton scattering, the γ-ray does not give all its energy to the electron. The photon scatters on the electron, transferring part of its energy. The scattered photon has a lower energy and can product other effects until it is absorbed. As a consequence, the measured energy spectrum will have a continuous distribution of energy, as shown in Fig.13.

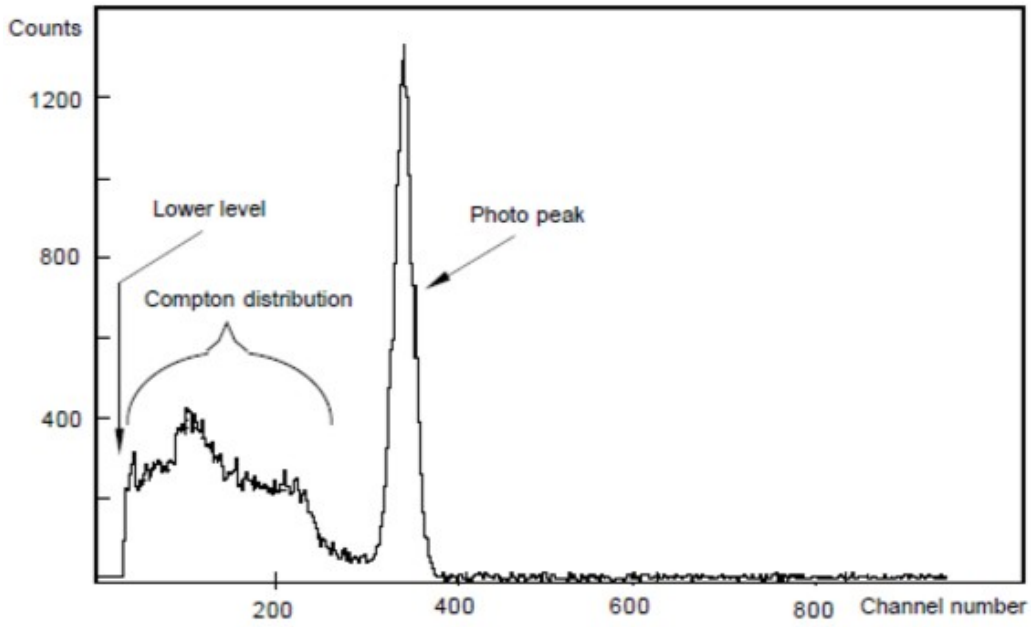

Fig. 13: Example of energy spectrum expected with photoelectric and Compton effects [19]. The energy of the photopeak is the same as the original γ-rays.

4.2.3 First Analysis

To start our analysis, we are going to look at data taken with a Cesium source placed next to the detector. We start with basic plots, using data given by the Basics Minitree of HAX (see the code and its comments in appendix).

In Fig.14 and 15, the colorbar shows the number of events. The first plot, Fig.14, is a x against y histogram (x and y are the position of the interaction on the TPC viewed from above). Fig.14 shows us that the most part of the events occurs on the right of the detector. We can see that the source was placed on the right of the detector. The second plot, Fig.15, is an energy spectrum of both S1 and cS1 signal. The x axis is in pe (photoelectron), unit proportional to the deposed energy in the PMTs: the more photons created and collected on the PMTs, the more photoelectrons are created in the photocatode. cS1 is the corrected S1 signal. It was corrected by the light collection efficiency map shown in Fig.11. The photopeak of cS1 is better defined than the photopeak of S1. In the cS1 energy spectrum, we can see the difference between the Compton edge and the photopeak but not on the S1 energy spectrum. The cS1 energy has a better resolution than the S1 energy. However, the energy resolution can be approved as we will see in part 4.3.

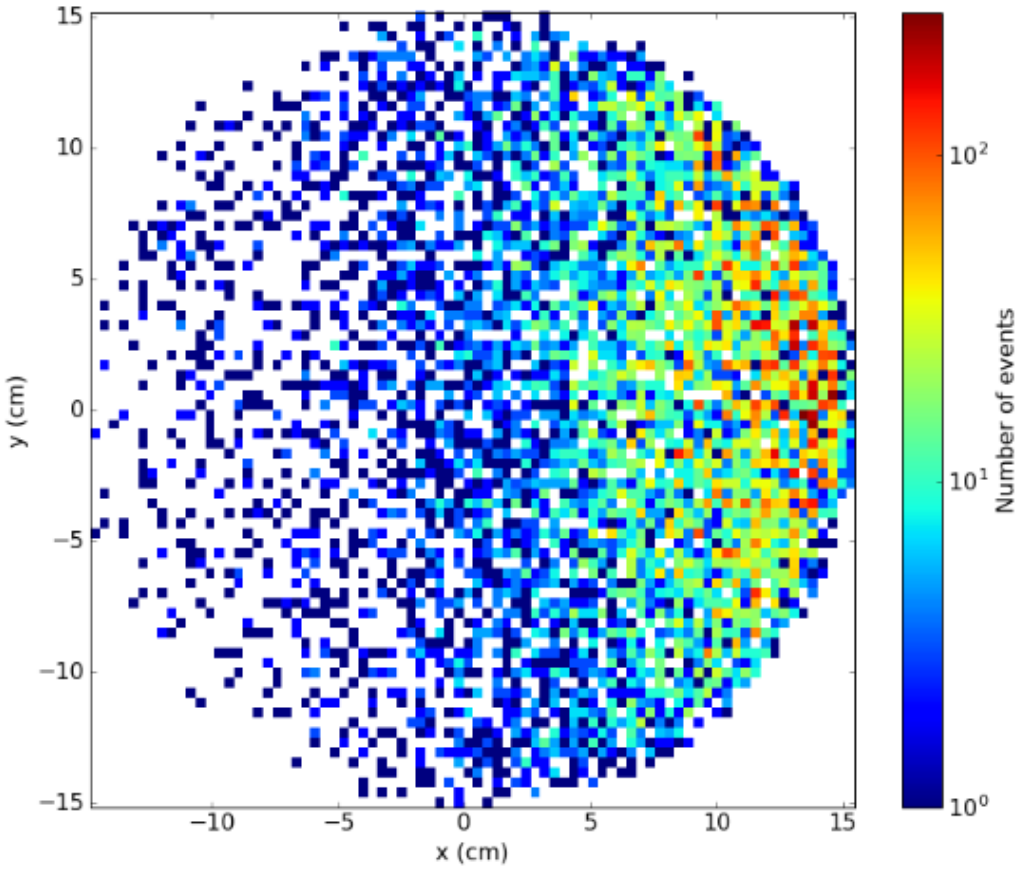

Fig. 14: x against y histogram, the number of events is showed by the colorbar. The Cesium source was on the right of the detector.

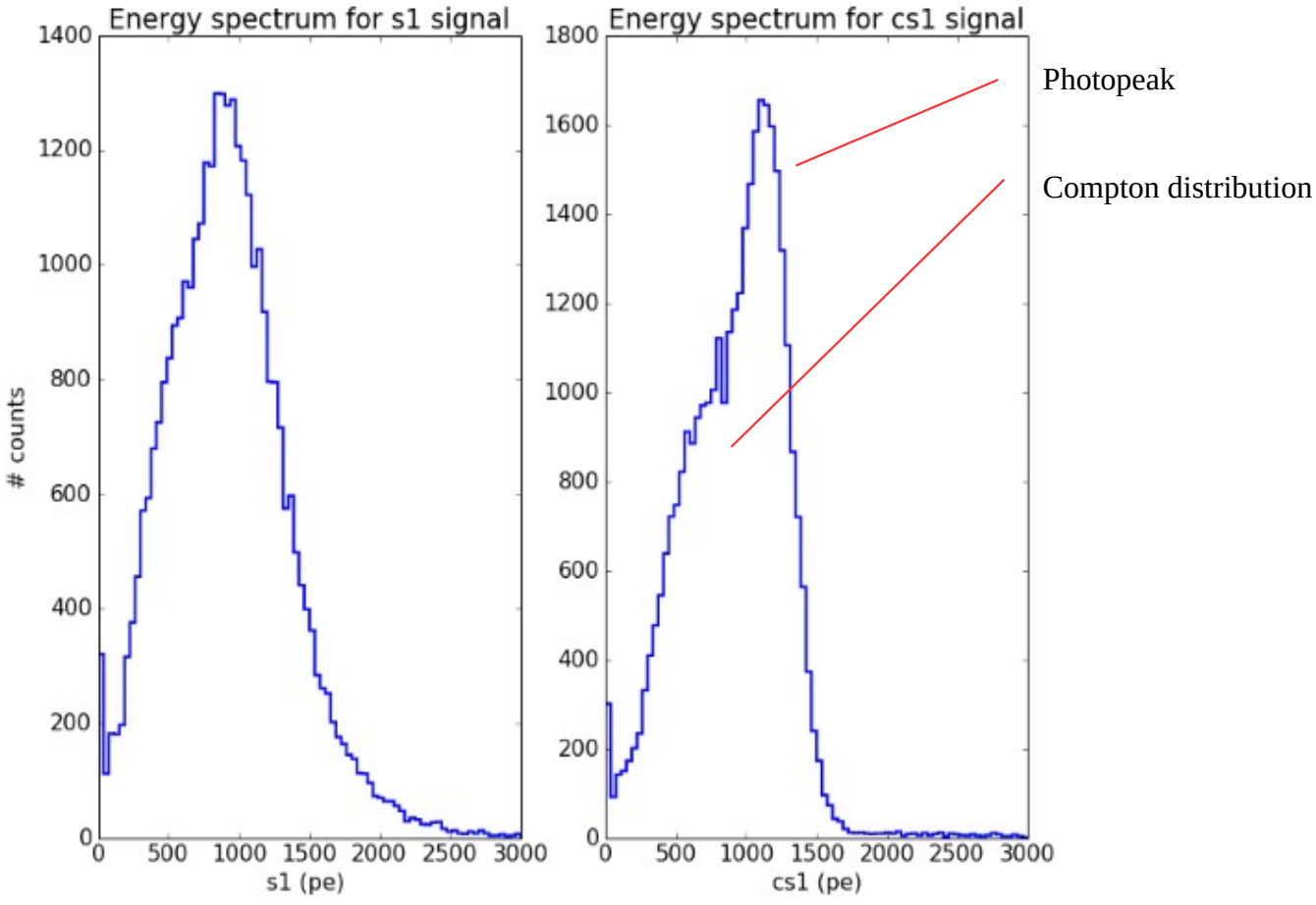

Fig. 15: Energy spectrum for S1 and cS1 signal (pe is for photoelectron). The Cesium photopeak can be seen in the cS1 spectrum.

4.3 Selection of events from the photopeak

To make a light collection efficiency map, the energy deposited in the TPC has to be precisely known. That is why we need to select events that only come from the photopeak, that means with a known energy of 662 keV.

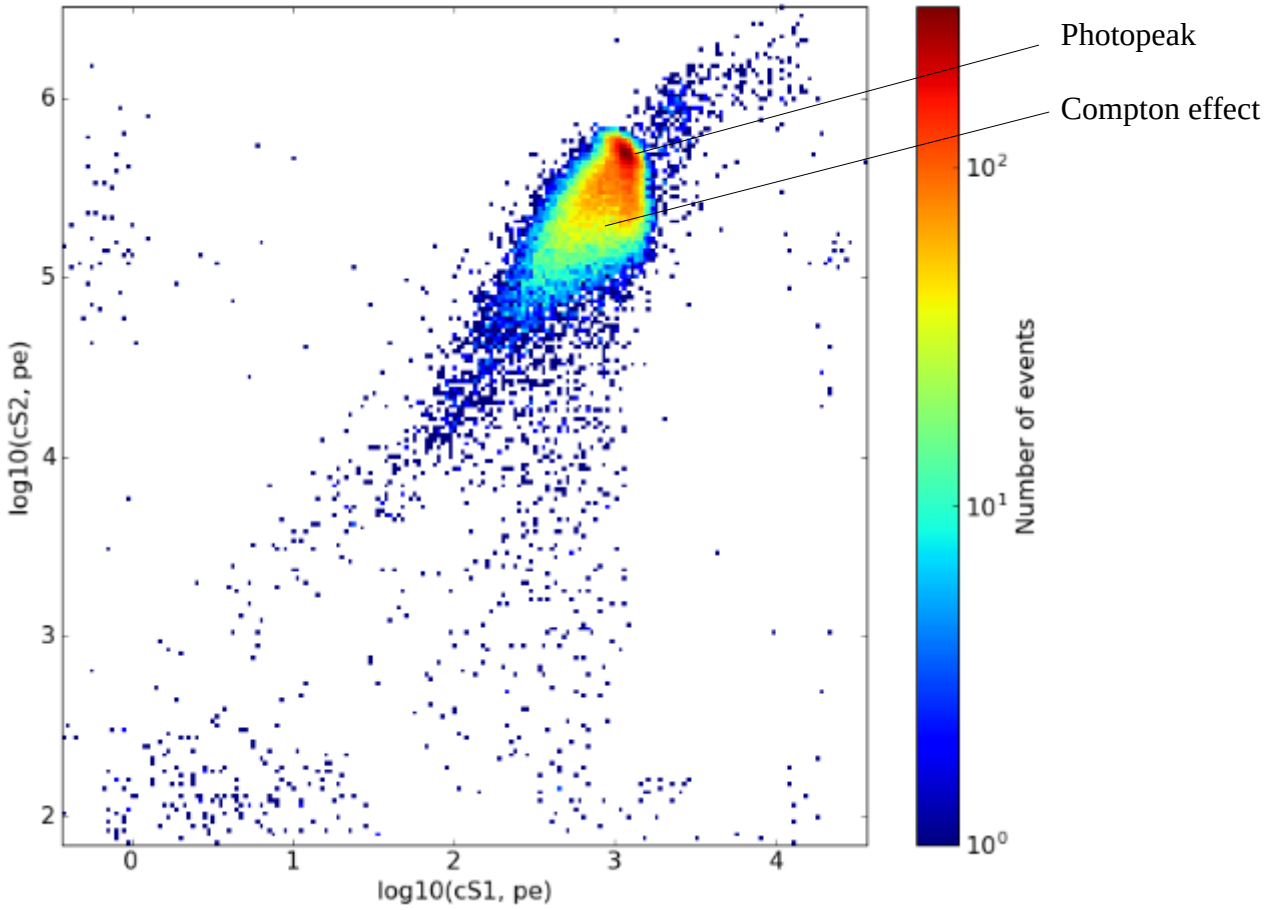

Fig. 16: cS1 against cS2 histogram (pe is for photoelectron). The photopeak is expected to be at the bin with the highest count.

Fig.16 shows the corrected signal S1 against the corrected signal S2, on a logarithm scale. In this pot, we can see a red “point” that indicates the bin with the highest amount of events: the photopeak. The rest of the event forms a “cloud” below the photopeak, due to the Compton scattering.

Now, we want to select only the photopeak's events. However, as seen in the precedent paragraph, the photopeak of the cS1 signal is broad: the energy resolution is low. Therefore, we can not used it to select photopeak's events. The same issue occurs for the cS2 signal. That is why, we are going to use the combined energy scale to improve the energy resolution.

4.3.1 The combined Energy Scale

S1 and S2 are anti-correlated. This anti-correlation is due to the fact that scintillation (S1) occurs after the excitation of a xenon atom, but also after the electrons coming the ionization recombine, as shown in Fig.17. However, S2 is proportional to the number of electrons that escape the recombination. In the presence of the electric field in the TPC, the number of electrons that escape the recombination increases, reducing the scintillation signal S1 and increasing the S2 signal. S1 and S2 signals are thus anti-correlated [20][21].

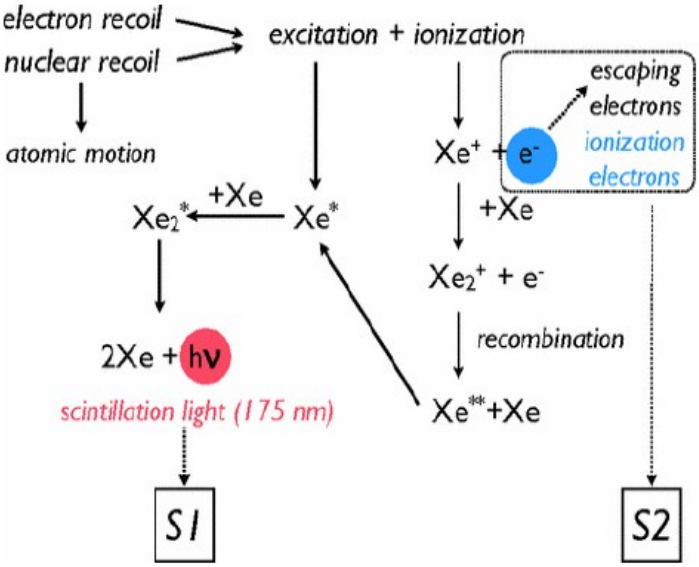

Fig. 17: Scintillation and ionization signals emission scenario [13]. The scintillation light (S1) is emitted after the excitation of xenon atoms and after the recombination of electrons coming from the ionization of xenon atoms. S2 signal is proportional to the number of electrons that escape the recombination.

In Fig.18, the S1 signal is shown proportional to light yield, and S2 signal to charge yield. If the drift field increase, the charge yield, and thus S2 signal, increases while the light yield, and thus S1 signal, decreases, showing that the proportion of S1 and S2 signals is different at different fields, but their sum, the combined energy scale, is constant (4.1) [22].

$$CES = a * S1 + b * S2 \tag{4.1}$$

To improve the energy resolution, we combine these two signals.

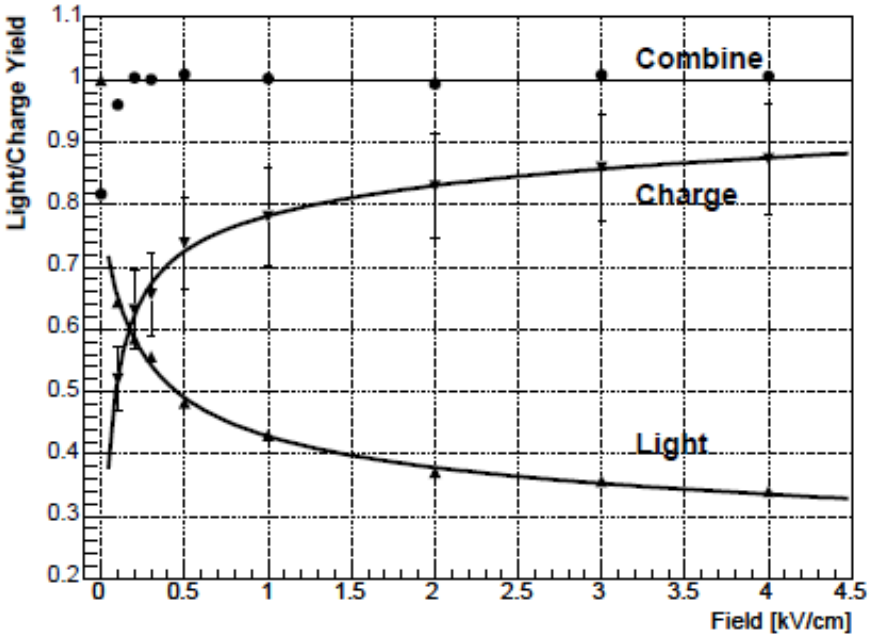

Fig. 18: Light and Charge yield as a function of drift field for 662 keV gamma-rays from Cesium 137 [22]. S1 is proportional to light and S2 is proportional to charge in liquid xenon.

4.3.2 The cS2 bottom signal

To calculate the combined energy scale, we use the "cS1" and "cS2_tot_bottom" signals, as shown in (4.2).

$$CES = a * cS1 + b * cS2\_tot\_bottom \tag{4.2}$$

cS2_tot_bottom is the corrected area of the S2 signal measured by the bottom array of photomultipliers. However, the Basic Minitree of HAX give us only the s2_area_top_fraction, that means the fraction of the area of the S2 signal measured by the top array of photomultiplier, and the cS2, that means the corrected area of the S2 signal, measured by both top and bottom PMTs array. Thereby, we can calculate cs2_tot_bottom based on (4.3).

$$cs2\_Tot\_bottom = (1 - s2\_area\_tot\_fraction) * cS2 \tag{4.3}$$

We use cS2_tot_bottom because it give a more precise energy than the cS2 signal, as shown in Fig.19. Indeed, the S2 signal is created near the top PMT array (in the gas phase), therefore, the saturation of the PMTs are more likely than if the signal was created further from the PMT array. When a PMT is saturated, the energy information is lost, given an imprecise measured energy.

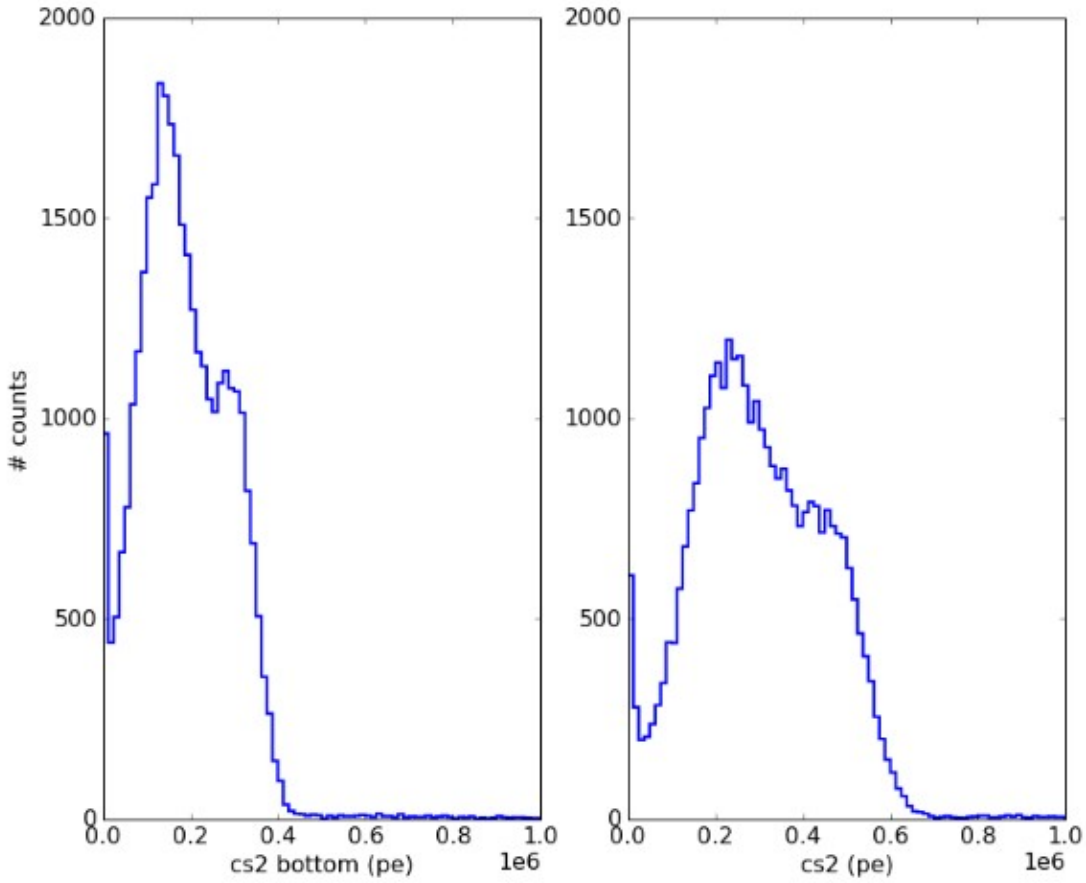

Fig. 19: Energy spectrum for cS2_tot_bottom and cS2 (pe is for photoelectron). cs2 bottom signal has a less broad energy spectrum than cS2 signal.

In Fig.20, we plot cS1 vs cS2_tot_bottom histogram. In this plot, we still see our photopeak which is expected to be at the bin with the highest count (approximately 700pe<cS1<1500pe and $2{,}5.10^5$pe<cS2_tot_bottom<4.10^5pe). However, we also clearly see an other population.

This population have approximately the same cS1 (1000pe<cS1<1500pe) but a lower cS2_tot_bottom (1.10^5pe<cS2_tot_bottom<2.10^5pe) than the population coming from photopeak.

The Fig.21 is an energy spectrum for cS2_tot_bottom and cS2 for regular and background data. In Fig.22 we compare cS1 vs cS2_tot_bottom with r^2 in colorbar for regular and background data. Based on these two plots, we can conclude that our unknown population is not due to background signal.

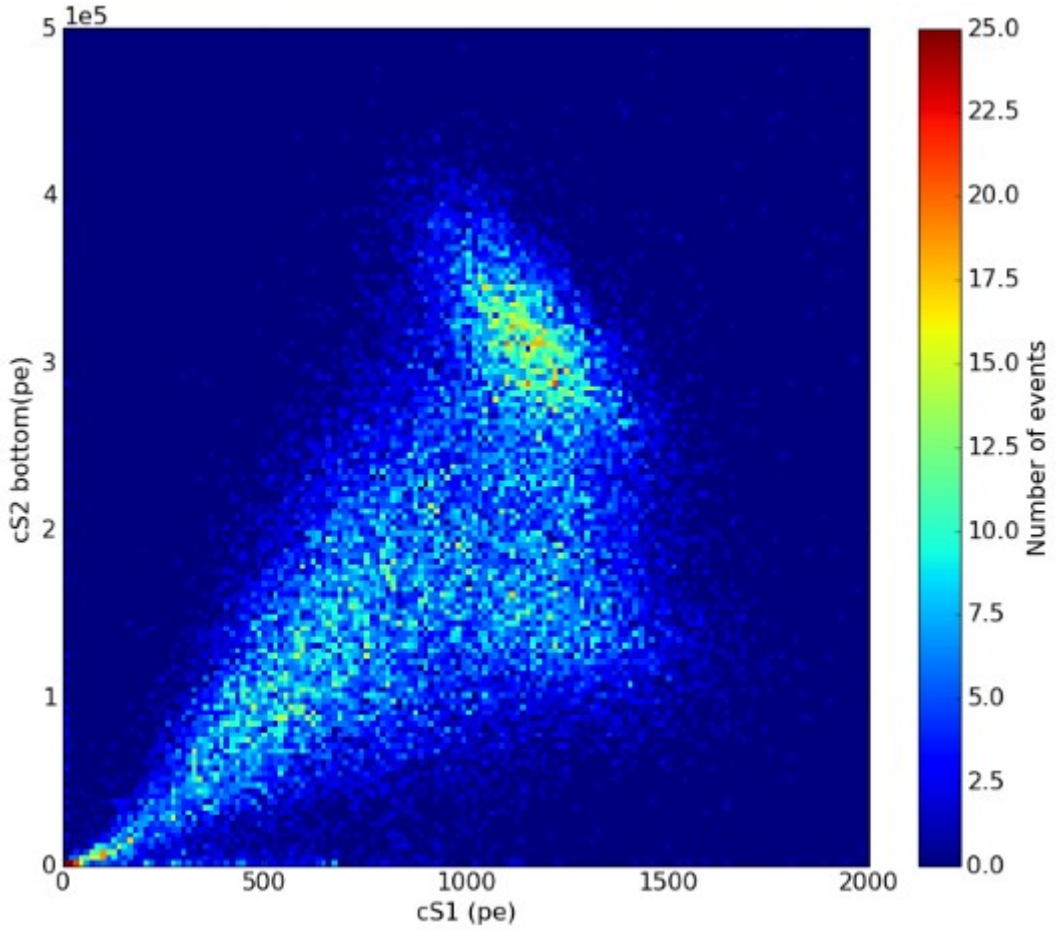

Fig. 20: cS1 against cS2_tot_bottom histogram. The number of events in shown on the colorbar. The photopeak is expected to be at the bin with the highest count.

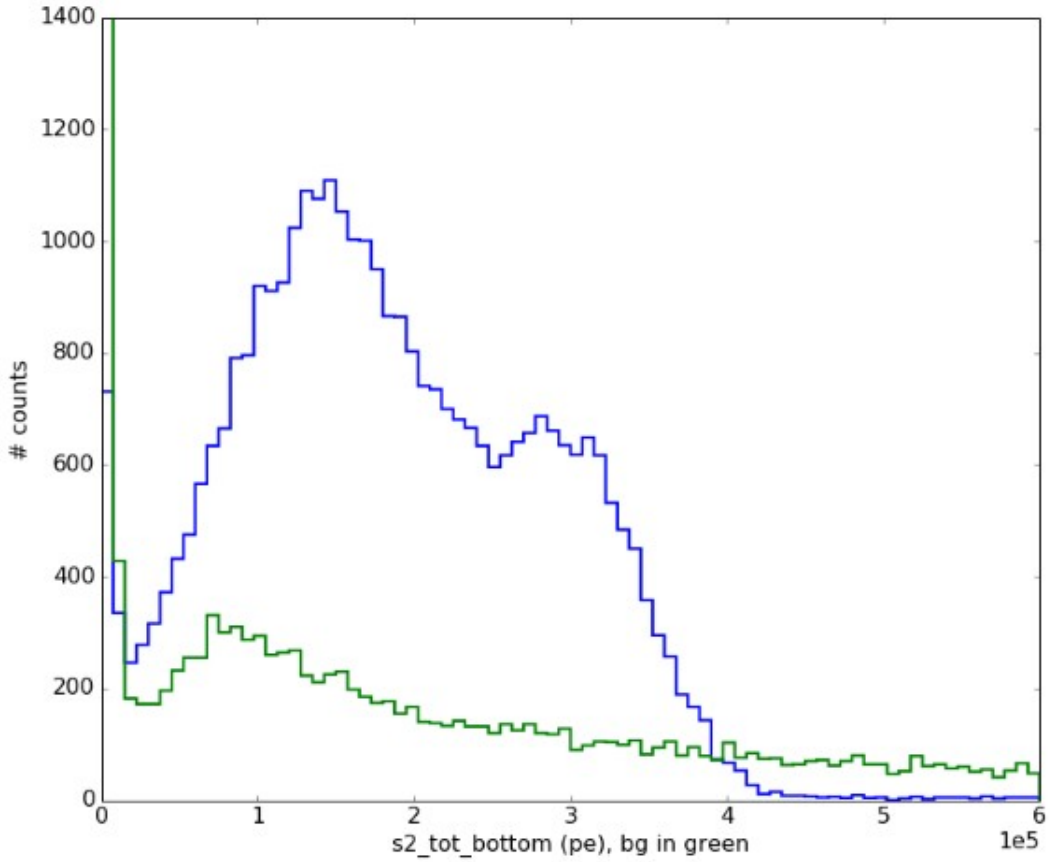

Fig. 21: Energy spectrum for cS2_tot_bottom in blue, compared to background signal in green (pe is for photoelectron). Background signal can not explain the unknown population.

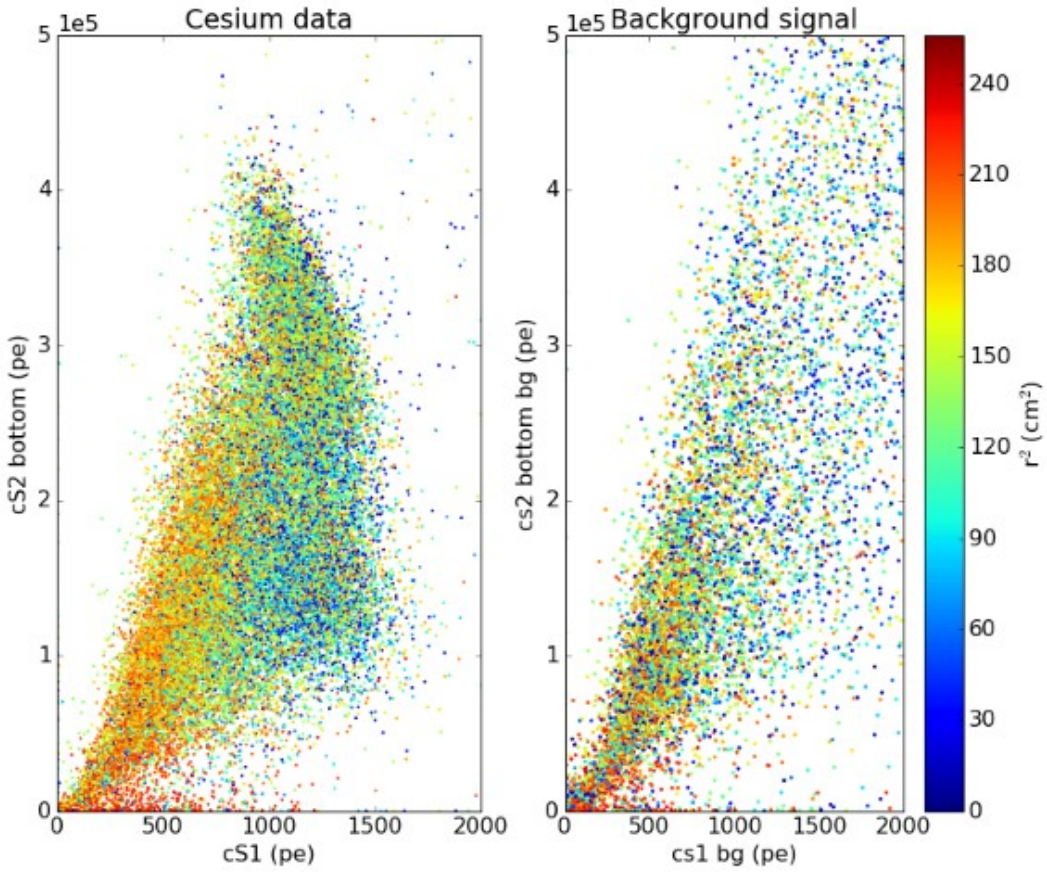

Fig. 22: cS1 against cS2_tot_bottom for regular data and background signal, r^2 is on the colorbar. Background signal can not explain the unknown population at 1000pe<cS1<1500pe and 1.10^5pe<cS2_tot_bottom<2.10^5. The unknown population is in the center of the TPC.

One hypothesis is that our unknown population is due to the double scatters events. When a Compton scattering happens, the original photon creates a S1 and S2 signal. Then, the scattered photon can also create another S1 and S2 signal. Both S1 signals are detected by the PMTs in the same time, since the speed of light in the TPC is higher than the detection speed of the PMTs. However, since the S2 signals are created after the travel of electrons, the PMT array will detect two S2 signals for one huge S1 signal. For PAX, only the biggest S2 signal corresponds to the measured S1 signal and is classified as a S2 signal. As a consequence, a large part of S2 signal are missed, given a population with a low S2 and a high S1.

If we cut this double scatters events from the data, the unknown population disappears, as shown in Fig.23. To do the cut, we use the “largest_other_s2”, which gives the energy of signals that look like S2 signals but are not classified as S2 signals. In the case of a double scatter event, the largest_other_s2 will be important, thus we cut events with a large largest_other_s2 (see appendix Cs137, we select event with largest_other_s2 <2000pe).

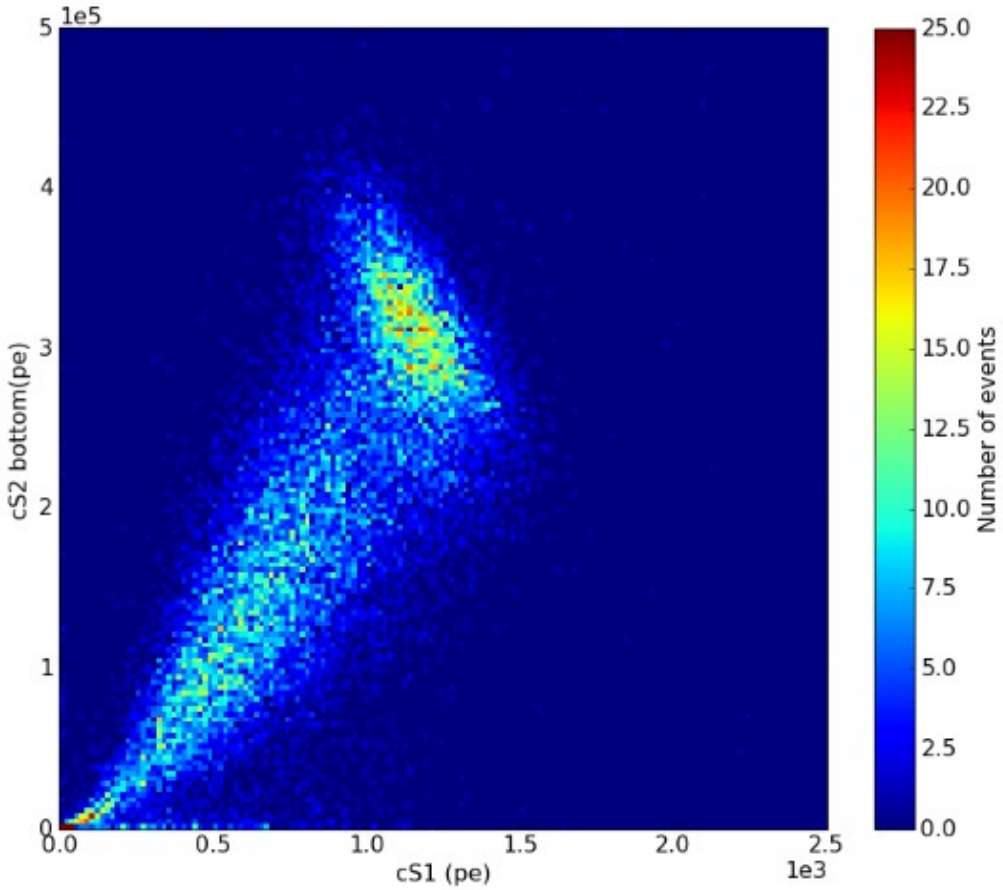

Fig. 23 : cS1 against cS2_tot_bottom histogram after the double scatters events cut, the number of events is showed in the colorbar. The unknown population is cut.

4.3.3 Determination of the combined energy scale

The combined energy scale is the projection of the cS1 and the cS2_tot_bottom energies along the large axis of the ellipse formed in the cS1 against cs2_tot_bottom plan. To do this projection, we need to determined the angle of anti-correlation between cS1 and cS2_tot_bottom. We fit a two dimensional Gaussian function to the data to select the ellipse, as shown in Fig.24, based on a code made by Erik Hogenbirk (see appendix, Cs137). The final combined energy scale (CES) is shown in Fig.25. We can see that CES have a better energy resolution than cS1 and cS2_tot_bottom (as shown in Table.1) and the photopeak is clearly defined, as intended.

Now, we can select events with a precise energy, compare this energy to the measured one and create a light collection efficiency map.

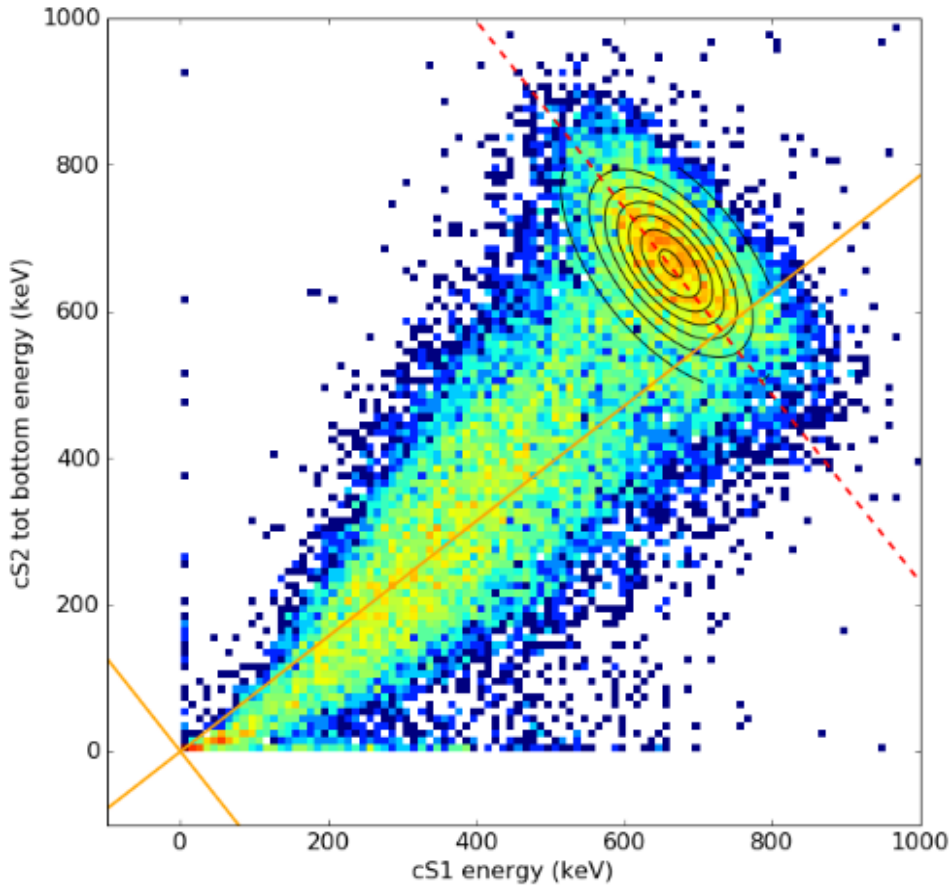

Fig. 24: Fitting of the data using a two dimensional Gaussian function. The combined energy scale is the projection of cS1 and cS2_tot_bottom energies along the large axis of the ellipse.

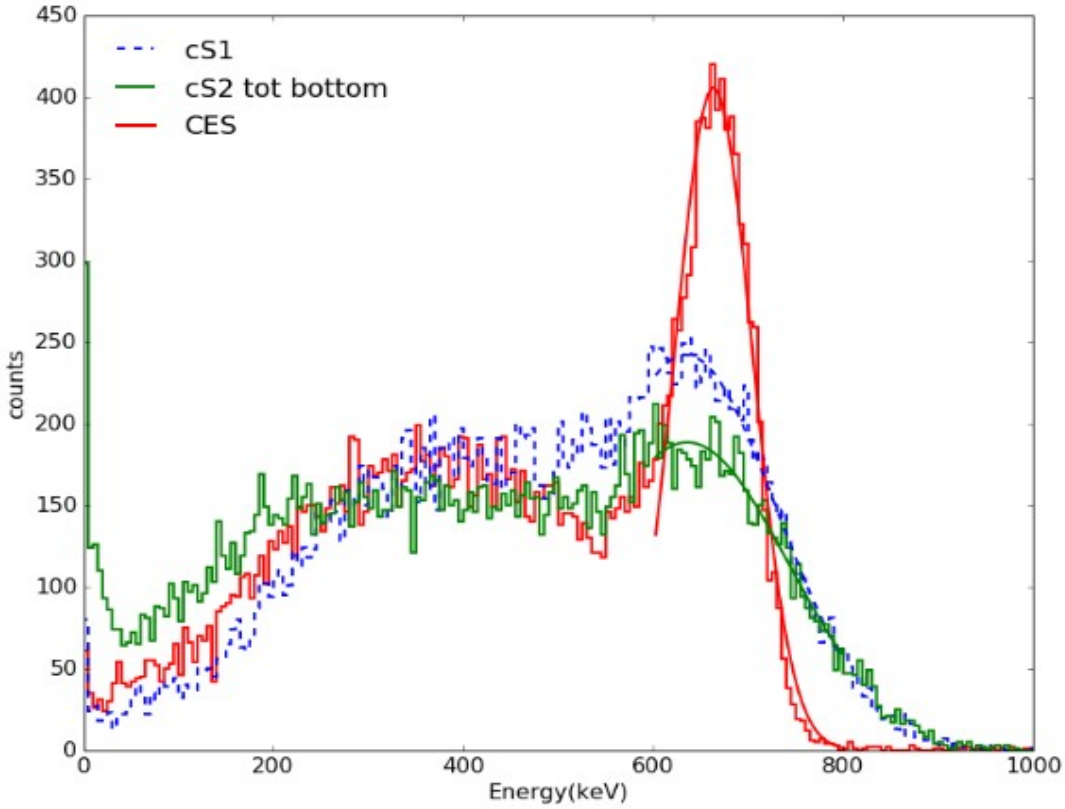

Fig. 25: Combined Energy Scale spectrum, compared with cS1 and cS2_tot_bottom spectrum. CES has a better energy resolution, we clearly see a Compton edge (from 150 keV to 600 keV) and a photopeak (at 662 keV).

Energy	Standard deviation σ (keV)	Energy Resolution (%)
CES	40,64	6,14%
cS1	103,98	15,71%
cS2_tot_botton	114,32	17,27%

Table 1: Standard deviation and energy resolution for CES, cS1 and cS2_tot_bottom. The standard deviation was determined by a fitting with a one dimentionnal gaussian function. The energy resolution is giving by : 662 (keV)/σ (keV) * 100. CES has the better energy resolution as intended.

In Fig.26, we select events coming from the photopeak, using the combined energy scale, and plot S1 against z and r^2, with $r^2=x^2+y^2$. These plots show us that the light collection efficiency of the S1 signal, for one given energy (here 662 keV), depends on the position of the interaction, proving that we need a light collection efficiency map to correct the data.

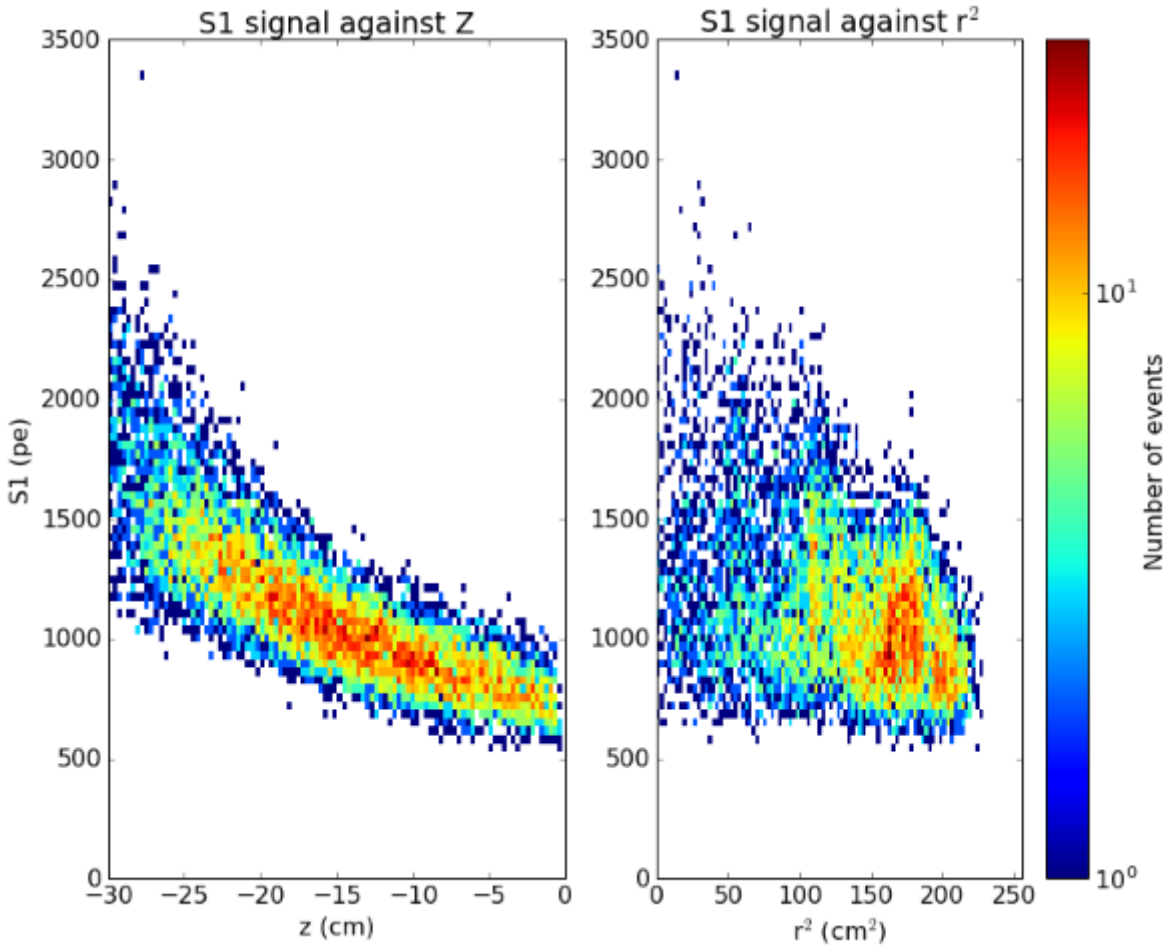

Fig. 26: S1 againts z and r^2 histogram, the number of event is showed by the colorbar. The quantity of measured light depends on the position of the interaction in the TPC.

4.4 S1 Light Collection Efficiency Map

To make a S1 Light Collection Efficiency map, we need more data with a large amounts of events coming from the photopeak and distributed throughout the detector. Since we use a large amounts of data, we have to make the processing faster by computing a Minitree that will cut events that are not in the photopeak, starting by a large square cut (see appendix, LCE map). Then, we calculate the combined energy scale, as shown in the previous paragraph, and select events with an energy of 662 keV. In Fig.27, we plot z against r^2 with S1 in colorbar after a selection of events that coming form the photopeak. We see that the light collection efficiency is maximal for an interaction in the center of the TPC and minimal for an interaction on the edge of the TPC.

The next step will be to create an overall light collection efficiency map, for all PMTs together. To do it, I will divide the TPC into spatial slices. In each slice, I will determine the relative difference between the measured S1 signal and the excepted one (that is means 662 keV), apply this map to the uncorrected S1 signal and try to recover the corrected signal cS1.

Finally, I will try to do the same procedure but for each PMTs individually. The difficulty of doing a map for each PMTs is that the LCE map depends on the position of the interaction but also on the position of the PMT. We need a per PMT light collection efficiency map to make a 3D position reconstruction on S1 signals that have no S2 signals and make a de-saturation correction for S1 signals (using the per PMT map to correct area of saturated PMTs).

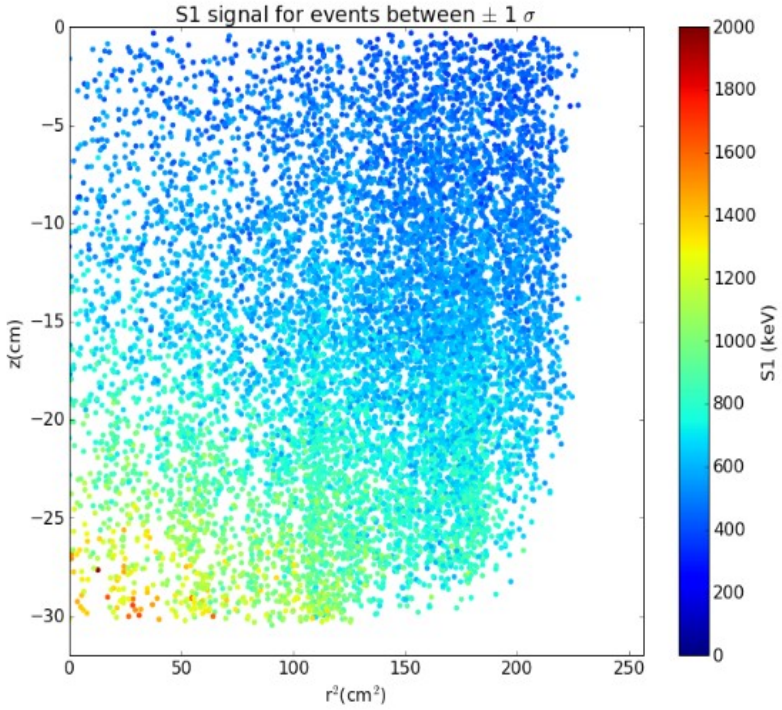

Fig. 27: z against r^2 plot. The colorbar shows the amount of measured S1 light. The maximum of light collection efficiency is reached for an interaction on the bottom center of the TPC (r^2~0 cm² and z~ -30 cm).

Conclusion

The purpose of my internship in Nikhef was to understand the data analysis of the XENON100 experiment, to improve the calibration of the detector with a Cesium source and make a light collection efficiency map of the XENON100 detector. I should, in the following 3 weeks, reach this last objective. First, I had to learn how data analysis software used in Nikhef, PAX, operated. Only then, I started working on data taken with a Cesium source placed next to the detector. Afterward, I determined the combined energy scale to improve the energy resolution of S1 and S2 signals and to select more precisely the event coming from the photopeak of the Cesium source. These events, with a precise energy of 662 keV, will allow me to create a light collection efficiency map of XENON100 detector.

This internship was a rewarding professional experience. While learning how to implement a scientific approach on the data analysis, it allowed me to discover the internal functioning of an international scientific collaboration. It also allowed me to improve my international skills, especially my scientific English, by talking about the XENON100 experiment with my colleagues, reading scientific articles, and doing oral presentations of my work in front of the dark matter group. I also had the opportunity to expand my computing skills, by learning a new programming language: Python.

Finally, this internship allowed me to glimpse the profession of researcher in experimental physics, and consolidate my professional project.

List of Figures

Bibliography

[1] BERTONE, Gianfranco, 2014, Le mystère de la matière noire, dans les coulisses de l'univers, Dunod, Quai des Sciences.

[2] Penn State: The rotation curve of the Milky Way: https://www.e-education.psu.edu/astro801/content/l8_p8.html

[3] BOUQUET, Alain, MONNIER, Emmanuel, 2003, Matière noire et autres cachotteries de l'univers, Dumod, Quai des Sciences.

[4] T.Marrodan Undagoitia, and Al. Hep-Ph(2015), arXiv:1509.08767, Dark matter direct-detection experiments, http://arxiv.org/pdf/1509.08767v1.pdf

[5] Jan Conrad and al., Hep-Ph (2014), arXiv:1411.1925, Indirect Detection of WIMP Dark Matter: a compact review, http://arxiv.org/abs/1411.1925

[6] ISAPP (Heidelbeg), Lectures, The Dark side of the Universe, Page 25, https://www.mpi-hd.mpg.de/lin/events/isapp2011/pages/lectures/de_los_Heros.pdf

[7] TAILLET, Richard, La matière noire: http://lapth.cnrs.fr/pg-nomin/taillet/dossier_matiere_noire/matiere_noire1.php

[8] M.Klasen, and al., Hep-Ph(2015), arXiv:1507.03800, Indirect and direct search for dark matter, http://arxiv.org/abs/1507.03800

[9] Subatech: La recherche de la matière noire: http://www-subatech.in2p3.fr/fr/recherche/nucleaire-et-sante/xenon/recherche/fondamentales/xenon100

[10] BAUDIS L. and al.,Astro-ph.IM (2012), arXiv:1203.1589v1, Results from the XENON100 Dark Matter Search Experiment: http://arxiv.org/abs/1203.1589

[11] Nikhef: https://www.nikhef.nl/en/science-technology/astroparticle-physics/donkere-materie/xenon-1t/#c1247

[12] Xenon Dark Matter Project: http://xenon.physik.uni-mainz.de/

[13] M. LE CALLOCH, thesis (2014), Study of the single electron charge signals in the XENON100 direct Dark Matter search experiment

[14] Web site: photomultiplier, http://psec.uchicago.edu/links/Photomultiplier_Handbook.pdf

[15] XENON100 Collaboration, astro-ph.IM (2012), arXiv:1107.2155, The XENON100 Dark Matter Experiment, http://arxiv.org/pdf/1107.2155.pdf

[16] XENON group notebooks: https://github.com/XENON1T

[17] BIN Choi, thesis (2013), The Light Response of the XENON100 Time Projection Chamber and the Measurements of the Optical Parameters with the Xenon Scintillation Light

[18] Wikipedia: Caesium 137, https://en.wikipedia.org/wiki/Caesium-137

[19] Web site: Gammadataeduction.ent: http://www.gammadata.net/sv/gammadata-utbildnings-webshop/utbildningsprodukter/faerdiga-laborationer-sv/measurement-of-a-gamma-ray-spectrum/

[20] EXO Collaboration, Hep-ex (2003), arXiv:0303008v1, Correlated Fluctuations between Luminescence and Ionization in Liquid Xenon, http://arxiv.org/pdf/hep-ex/0303008v1.pdf

[21] A. BEHRENS, thesis (2014), Light Detectors for the XENON100 and XENON1T

[22] XENON Collaboration, Astro-ph (2007), arXiv:0704.1118v1, Observation of Anti-correlation between Scintillation and Ionization for MeV Gamma-Rays in Liquid Xenon, http://arxiv.org/pdf/0704.1118v1.pdf

Appendix

You can find the commented code that I made to do this data analysis in the following link:

https://github.com/ChloeTh/MasterProject

- Master project Cs137: code for the first data analysis and the combined energy scale computing:

https://github.com/ChloeTh/MasterProject/blob/master/MasterProject%20Cs137.ipynb

- Master project LCEmap1: start of the light collection efficiency map computing:

https://github.com/ChloeTh/MasterProject/blob/master/MasterProjectLCEMap1.ipynb